The lipid kinase PI3Kα is required for aggregation and survival of ovarian intraperitoneal cancer cells.

Authors

Thole A [1,2], Thibault B [1,2], Basset C [1,2,3], Guillermet-Guibert J [1,2]*.

1: INSERM – UMR 1037 – Team 17, 2 avenue Hubert Curien; Oncopole de Toulouse. Toulouse, France.

2: LABEX TouCAN. Toulouse, France.

3: Service d'Anatomo-Pathologie, Institut Universitaire du Cancer de Toulouse – Oncopole (IUCT-O), avenue Irène Joliot-Curie. Toulouse, France.

***corresponding author:** Julie Guillermet-Guibert

CRCT UMR1037 INSERM-Université Toulouse 3 - ERL5294 CNRS; 2 avenue Hubert Curien; Oncopole de Toulouse; CS 53717; 31037 TOULOUSE CEDEX 1 - FRANCE

Tel : +33 (0) 5 82 74 16 52

E-mail: julie.guillermet@inserm.fr

http://www.crct-inserm.fr/17-j-guillermet-guibert-sigdyn-group-pi3k-isoforms-signalling-cancerogenesis-559.html

http://eupancreas.com/julie-guillermet-guibert

http://pi3k-phdproject.eu/partner/julie-guillermet-guibert/

Running Title

PI3Kα controls tumour cell aggregation

SUMMARY (241 WORDS) - MAX 250 WORDS

Objective: Peritoneal carcinomatosis in ovarian cancer is often associated with ascites. Because of the emerging concept that multicellular cell growth conditions can lead to increased resistance to conventional therapies, we investigated the importance of PI3Kα-driven pro-tumorigenic and pro-chemoresistance signals in the formation of a 3D model of ovarian cancer ascites. **Methods:** We retrospectively analysed tumour cell aggregation and ascites composition in ovarian cancer adenocarcinomas at diagnosis with patient survival clinical data, then set up an ex-vivo 3D model. PI3K inhibition covered the full pharmacological arsenal available to target PI3K activity (pan-PI3K or isoform-selective inhibitors). We quantified cell survival, metabolism and cohesion of multicellular aggregates after treatment with PI3K inhibitors and/or cisplatin. **Results:** In malignant ascites, isolated tumour cells and cell aggregates were present with variability in size and number and aggregate-poor ascites predicted a poorer survival of ovarian adenocarcinoma patients. Ex-vivo patient-derived cell culture with the addition of mesenchymal stem cells, as a model of tumoural stroma, favoured aggregation of tumour cells. We demonstrated, by use of selective inhibitors of the PI3Kα isoform, its key role in the formation and maintenance of multicellular aggregates. This role did not depend solely on a pro-survival activity of PI3Kα but could be linked to changes in cell/cell adhesion. Finally, PI3Kα-selective inhibitors were also equally efficient in the presence of cisplatin. **Conclusion:** We have identified a signalling pathway of interest for the treatment of advanced ovarian cancer, which could limit the progression of this cancer.

Key words

PI3K signalling, tumour cell aggregation, resistance to treatment, signal-targeted therapies, malignant ascites

3958 words (4000 words max)

INTRODUCTION

Worldwide, ovarian cancer is ranked eighth in cancer incidence, but fourth in female mortality [1]. It is often associated with a poor prognosis due to the frequent intraperitoneal implantation of tumour cells, called peritoneal carcinomatosis, observed at advanced stages [2]. Found in around 89% of patients with stage III or IV ovarian cancer, massive production of ascites fluid (inflammatory exudate present in the peritoneal cavity) is in most cases associated with peritoneal carcinomatosis [3]. Unlike most solid cancers, ovarian cancer cells rarely migrate haematogeneously, but instead can disseminate by direct extension to neighbouring organs, especially via the transcoelomic pathway. By this mechanism, cancer cells detach from the primary tumour and are then passively transported by the fluid of the peritoneal cavity that is in proximity to the entire wall of the peritoneum and omentum, allowing the development of peritoneal carcinomatosis at multiple foci [2,4,5].

Twenty years ago, peritoneal carcinomatosis was seen as an incurable pathology requiring palliative care only. However, the introduction of loco-regional therapies combining cytoreductive surgery with hyperthermic intraperitoneal chemotherapy (HIPEC) based on platinum salts or taxanes changed the management of this disease [6]. Signal-targeted therapies, such as those targeting the PI3K (phosphoinositide 3-kinase)/Akt pathway, are currently being tested in these patients with the goal of improving disease-free survival rates [7].

Tumour cell resistance to chemotherapy is now largely considered to be enhanced in multicellular three-dimensional (3D) structures. For example, EMT-6 mammary tumour cells are more resistant to alkylating agents (cyclophosphamide, cisplatin, thiotepa) when grown in 3D spheroids [2,8]. Single or clustered cells can detach from breast or prostate primary tumours and can then be found in the bloodstream [9]. In the peritoneal cavity, the formation and properties of

these peritoneal tumoural aggregates remain poorly understood. It is also largely accepted that peritoneal microenvironment contributes to resistance to chemotherapy [10], in particular via mesenchymal stem cells (MSCs) [11]. They have been shown to contribute to tumour cells' ability to form spheroids called tumorospheres under anchorage-independent culture conditions, increasing their capacity to induce tumour formation in vivo after mouse xenografts [12,13].

The class I PI3K/Akt axis is one of the most commonly deregulated pathways in cancers, particularly in ovarian cancer. There are four heterodimeric isoforms of class I PI3K in vertebrates: α, β, γ and δ. PI3K activation results in the phosphorylation of phosphatidylinositol 4,5 biphosphate (PIP2) into PIP3, which acts as a second messenger in the cell. Downstream signals of PI3K, including the members of the Akt/mTOR (mammalian target of rapamycin) pathway, are numerous and involved in many cellular processes, including cell-cycle progression and actin cytoskeleton rearrangement [14–17]. Activation of the PI3K pathway is associated with increased migration and invasion of different subpopulations of ovarian cancer cells, making this signalling pathway a predictor of the invasive and migratory potential of ovarian tumour cells [18]. Mutations are found in the *PIK3CA* gene encoding PI3Kα in 6–33% of patients, and amplification or copy gain of this gene are found in 13–39.8% of cases [19]; these alterations are non-exclusive. Regarding the distributions of these alterations in the different subtypes of ovarian carcinomas, *PIK3CA* mutations are less common in high-grade serous carcinomas, while amplifications are frequently observed. The genetic landscape of ovarian carcinomas suggests that PI3K inhibitors, and in particular those targeting PI3Kα, could be tested in this pathology. A PI3Kα-selective inhibitor, BYL719 (Alpelisib), has just been approved for use in breast cancer [20,21], and BYL719 in combination with oestrogen receptor inhibitors show lower toxicity compared to the use of pan-PI3K inhibitors. The importance of PI3Kα activity in tumoural aggregates with an ovarian origin is unknown.

Our objective is to validate a model of ovarian cancer cell aggregates and associated ascites and demonstrate the involvement of PI3Kα during transcoelomic tumorosphere formation and maintenance.

MATERIAL AND METHODS

Patient ascites-derived cell tumorospheres

Ascites fluids were taken from patients with ovarian cancer after consent (CRB Cancer des Hôpitaux de Toulouse, IUCT-O, Toulouse – BB-0033-00014, DC-2008-463, AC-2013-1955). Supplementary Table S1 details patient information; clinical and biological annotations of the samples have been declared to the CNIL (Comité National Informatique et Libertés).

Cell lines, 3D culture, treatments and phenotypic analysis

SKOV-3-GFP cells correspond to genetically modified SKOV-3 wild-type (WT) cells expressing GFP (green fluorescent protein). MSCs were derived from healthy donors who underwent hip surgery (Etablissement Français du Sang). Cells were cultured at 37°C, 5% CO_2 under a humid atmosphere, in RPMI 1640 medium (Sigma) for SKOV-3 cells and DMEM (Sigma) for MSCs; 50% of each medium was used when the two cell types were mixed. The culture medium was supplemented with 10% FCS (foetal calf serum), 1% L-glutamine, 1% penicillin-streptomycin and 0.01% plasmocin (Invitrogen).

One thousand patient-derived tumoural cells or SKOV-3-GFP and SKOV-3 WT cells, with or without increasing numbers of MSCs, were seeded in round bottom 96-well plates (Nunclon Sphera, ThermoFisher Scientific). Living cell numbers and metabolic activity were measured with an MTT assay, the alamarBlue™ (Invitrogen) or CellTiter-Glo assay (Promega) or labelled for 1 h using the LIVE/DEAD® kit (ThermoFisher Scientific) containing 2 µM calcein and 4 µM EthD-1 (Ethidium homodimer-1). Cell clusters obtained were observed and imaged with an AxioVert microscope on days 1, 4, 7, 10 and 14 using ZEN® software (Carl Zeiss). The

same software measured their diameter and surface. For each condition, triplicates were performed and the average area was compared to the day 1 average of the corresponding experiment (representing 100% of the area). Western blotting was performed as described in [14] with the following antibodies:

Primary antibody	Origin	Dilution	Provider	Size	Secondary antibody
pAkt (S473)	Rabbit	1/1000	Cell signaling #4060	60kDa	1/3300
pAkt (T308)	Rabbit	1/1000	Cell signaling #4056	60kDa	1/3300
Akt total	Rabbit	1/1000	Cell signaling #4691	60kDa	1/20 000
pCofilin (S3)	Rabbit	1/1000	Cell signaling #3313	19kDa	1/3300
Cofilin	Rabbit	1/1000	Cell signaling #5175	19kDa	1/20000
β-Actin	Mouse	1/2000	Sigma Aldrich AC74	42kDa	1/10 000

Pharmacological inhibitors

Treatments used in this study were as follows: Cisplatin (kindly supplied by Institut Universitaire du Cancer – Oncopole (IUCT-O), A66 (Axon Medchem) PI3Kα inhibitor (in vitro IC50 in nM: p110α: 32; β: >12500; δ: >1250; γ: 3480) [22]; BYL719 (Apex Bio) PI3Kα inhibitor (in vitro IC50 in nM: p110α: 4.6; β: 1156; δ: 290; γ: 250) [23]; TGX-221 (Axon Medchem) PI3Kβ inhibitor (in vitro IC50 in nM: p110α: 5000; β: 5; δ: 100; γ: 10000) [24]; AZD8186 (MedChemExpress) PI3Kβ/δ inhibitor (in vitro IC50 in nM: p110α: 35; β: 4; δ: 12; γ: 675) [25].

Qdot® cell labelling of MSCs

Labelling was performed according to the supplier's recommendations, with the equimolar mix of the labelling kit at dilution 1/100 incubated for 1 h at room temperature applied directly to the cell cultures for 45 minutes.

Statistics

Quantitative variables are presented by means and qualitative data by percentages. Group comparisons were made using the ANOVA test (matched data) and the Student's t-test for parametric tests. For all experiments, a statistical difference is reached for $p<0.05$.

RESULTS

Peritoneal tumour cells from ascites biopsies form aggregates whose growth is delayed by a high number of initial cells

Ascites were biopsied and analysed to detect the presence of ovarian adenocarcinomatous cells. We first described the tumour cell aggregates found in ascites associated with ovarian adenocarcinomas in patients; aggregates were identified by use of cytospin and embedded preparation with standard immunohistochemical analysis with Papanicolaou, May-Grünwald-Giemsa, periodic acid–Schiff and epithelial cell adhesion molecule staining (Fig. 1A). Most ascites (11/12 patients) were composed of limited numbers of isolated tumoural cells and numerous aggregated tumoural cells (Fig. 1A). Only one case revealed numerous isolated cells alongside aggregates. We observed heterogeneity in terms of the distribution of cellular aggregate density; patients with aggregate-rich ascites had better survival compared to patients with aggregate-poor ascites (Fig. 1B, Suppl. Table S1). When grown in 3D-favourable conditions, ascites cells formed dense spheroids (Fig. 1C). To better reproduce peritoneal carcinomatosis development of transcoelomic aggregates (Fig. 1D), we first developed a 3D culture system of peritoneal tumour cells expressing GFP derived from the ovarian cancer cell line SKOV-3 (Fig. 1E). After 14 days, we analysed the influence of cell numbers in aggregates and observed an increase of 75% and 13% in the tumorosphere area when 5,000 and 10,000 cells were seeded, respectively (Fig. 1F). A higher number of initial cells appears to slow tumorosphere growth (Fig. 1E and F). Interestingly, area evolution (+24% in 7 days) (Fig. 1F) correlated with expression of

fluorescent GFP (+6% in 7 days), indicative of transcriptional/translational cellular activity (Fig. 1G, left), and metabolic activity indicative of cell survival (+29% in 7 days) (Fig. 1G, right). We then carried out 3D cultures with 10,000 MSC and observed a completely different aggregate evolution profile compared to SKOV-3 cells; there was very fast cell aggregation the day after seeding, and within 14 days the aggregate area had decreased by more than 60% compared to the initial area (Suppl. Fig. S1A and B). We also observed formation of fibrous-like structures within MSC aggregates, the nature of which remains to be determined (Suppl. Fig S1C). We then co-cultured 5000 GFP-expressing SKOV-3 cells with different quantities of Qdot-labelled MSCs as a model of stromal cells found in ascites (Fig. 1H and Suppl. Fig. S1D–F) [26]. The heterotypic tumorosphere area decreased proportionally to the number of MSCs, with an apparent increased cohesion (Fig. 1H). GFP fluorescence corresponding to tumour cells did not vary regardless of MSC number, indicating that these cells induced tumorosphere compaction without modifying tumour cell proliferation (Suppl. Fig. S1D and E). At a high ratio of MSCs to tumour cells, MSCs clustered in the centre of tumorospheres and colocalized with tumour cells (yellow staining, Suppl. Fig. S1F).

These results reveal that small-sized tumorospheres exhibit cellular growth and that the addition of MSCs to tumour cell spheroids results in increased compaction of tumorospheres, reminiscent of the observed formation of tumorospheres from patients' ascites cells.

PI3Kα inhibition prevents formation of ovarian cancer cell tumorospheres.

The PI3K/Akt pathway plays a role in cell proliferation and survival but is also involved in regulation of the actin cytoskeleton, suggesting a role in tumorosphere formation [14,16,17]. To determine the action of this pathway in the formation of SKOV-3-GFP multicellular aggregates, we treated them at seeding and 3 days later with the PI3Kα-selective inhibitors A66 and BYL719 (Fig. 2A). We confirmed a concentration-dependent inhibition of Akt

phosphorylation on S473 and T308 after A66 and BYL719 treatment (Fig. 2B–D), indicating 1) that the PI3K pathway is constitutively activated in SKOV-3 cells, 2) that this activation is highly dependent on the PI3Kα isoform and 3) that the pharmacological agents used prevent its activity.

We next compared the efficiency of a low (1 µM) and medium (10 µM) dose of PI3K inhibitors; in clinical trials, plasma concentrations of BYL719 are around 50 µM [27]. After 4 and 7 days of treatment with 10 µM of BYL719, we observed a complete reduction of the tumorosphere area and a total loss of fluorescence (Fig. 2E–G). Aggregates treated with 10 µM of A66 or 1 µM of BYL719 had comparable evolution profiles (Fig. 2E) with a decrease in tumorosphere area of about 30% compared to the control at day 4 (Fig. 2F). We compared our results to the standard treatment of ovarian cancer, cisplatin, at doses found in patients (0.5 µM and 5 µM); 5 µM is close to a dose causing patient toxicity [28]. A total disruption of SKOV-3 tumorospheres was observed only at high concentrations and after 7 days of treatment (Fig. 2H–J). Hence, we observed a significant alteration of tumorosphere cohesion, tumorosphere area (Fig. 2E–F) and cellular activity (Fig. 2G) at low doses of the PI3Kα inhibitor, which was never seen with low doses of cisplatin (Fig. 2I–J). This effect was maintained over time.

These results suggest that PI3Kα inhibitors can reduce tumorosphere formation while having a cytotoxic effect on aggregated or non-aggregated cells in a dose-dependent manner, whereas cisplatin appears to have cytotoxic effects only in a delayed manner and at a high concentration that is close to a dose causing patient toxicity.

PI3Kα selective inhibition prevents maintenance of ovarian cancer cell tumorospheres.

To measure PI3Kα inhibitor effects on tumorosphere maintenance, we treated already established SKOV-3-GFP cell aggregates (Fig. 3A).

PI3Kα inhibitors caused a concentration-dependent decrease in tumorosphere area and a tumorosphere morphology change corresponding to a decrease in compaction with maximal effect

at day 7 (Fig. 3B–D). Used at 1 μM, treatment with BYL719 resulted in a greater effect than A66; there was a significant decrease in tumorosphere area of 86% and 43%, respectively, compared to the vehicle at day 7 (Fig. 3C and D). This corresponded to a decrease in the initial size of tumorospheres. Treatment with TGX-221, a PI3Kβ-selective inhibitor, did not significantly modify tumorophere morphology (Fig. 3B) or area (Fig. 3E) compared with vehicle treatment, although there was a tendency towards an increase in area. AZD8186, a PI3Kβ/δ dual inhibitor, used at 1 μM, only resulted in a significant decrease of 38% in tumorosphere area after 7 days of treatment, corresponding to an arrest in tumorosphere growth (Fig. 3F).

Cisplatin treatment reduced tumorosphere area by 38% compared to the vehicle only after 7 days of treatment with a high concentration of 5 μM (Fig. 3G–H); 0.05 and 0.5 μM did not prevent tumorosphere growth observed at day 7.

PI3Kα inhibitors cause a decrease in the area of existing tumorospheres in an α isoform-specific manner.

Only PI3Kα inhibition impacts ovarian tumour cell viability in 3D culture.

We next aimed to determine the impact of the 3D culture on tumour cell resistance to cisplatin, the standard treatment for ovarian peritoneal carcinomatosis. We treated SKOV-3-GFP cells cultured in 2D or in 3D with PI3K inhibitors or cisplatin. In 2D, the two PI3Kα inhibitors showed a concentration-dependent cytotoxic effect on SKOV-3-GFP cells from a concentration of 1 μM (Fig. 4B). With cisplatin, a significant decrease in living cell numbers was only observed for concentrations ≥3.25 μM (Fig. 4C). In 3D, only PI3Kα-specific inhibitors showed a cytotoxic effect on SKOV-3 tumorospheres at a high concentration of 10 μM (Fig. 4D). Cisplatin and PI3Kβ inhibitors did not modify the number of living cells in 3D (Fig. 4D and E).

Unlike cisplatin, PI3Kα inhibitors retained a concentration-dependent effect (although not significant) at day 4 (Suppl. Fig. S2A and B). The cytotoxic effect of cisplatin observed in 2D was

therefore abolished by 3D culture, whereas PI3Kα inhibitor treatment still showed cytotoxic effects, albeit diminished, in tumorospheres (Fig. 4B–E).

To further analyse organization and distribution of living and dead cells within tumorospheres under treatment, we labelled living cells in green (calcein) and dead cells in red (EthD-1). First, we quantified the living cell areas using calcein staining (Fig. 4F–H) and demonstrated that BYL-719 significantly decreased this marker of living cell (Fig. 4G and H). SKOV-3 cell treatment with PI3Kα inhibitors altered tumorosphere cohesion and tended to increase the number of dead cells (Suppl. Fig. S2C). Only 10 μM of BYL719 caused a significant decrease in the living cell area (Fig. 4F and G). As observed previously, a 0.5 μM cisplatin concentration did not modify morphology of aggregates. Tumorosphere disintegration and a decrease in living cell area was only detected after 7 days with 5 μM of cisplatin treatment (Fig. 4F, H). As previously observed, PI3Kα inhibitors induced a rapid decrease in tumorosphere cohesion and viability (Fig. 4F and G, Suppl. Fig. S2) compared to cisplatin, which resulted in tumorosphere disintegration only at a high concentration and after 7 days of treatment (Fig. 4F and H).

Regarding the localization of living and dead cells, untreated SKOV-3 tumorospheres appeared to have a dead cell inner core; treatment with PI3Kα inhibitors suppressed this core, with dead cells observed throughout the whole area of the tumorosphere, particularly in the outer layer (Suppl. Fig. S2C). As observed previously, the PI3Kβ-specific inhibitor TGX-221 at 1 μM did not alter SKOV-3 WT tumorosphere morphology (Fig. 4F) and area (Fig. 4G). At a high concentration (a concentration at which selectivity towards PI3Kβ and other members of the PI3K family has not been demonstrated), we observed an unexplained increase in the living cell area despite a loss of cohesion (Fig. 4F), combined with a decreased number of inner dead cells compared to other PI3Kβ-targeting inhibitors at similar concentrations (Suppl. Fig. S2C).

AZD8186 only slightly modified the area of living cells (Fig. 4G) but seemed to alter tumorosphere morphology by altering their cohesion at both concentrations assessed (Fig. 4F).

Despite a decreased effect in 3D culture, PI3Kα inhibition is more effective is more effective at inducing tumorosphere disaggregation than cisplatin.

PI3K inhibitors decrease tumorosphere survival in the presence of cisplatin.

If used in the clinic for the treatment of ovarian cancer, PI3K inhibitors will be tested in combination [27]. A combination of a low concentration of cisplatin with PI3Kα inhibitors appeared to alter more efficiently SKOV-3-GFP tumorosphere morphology, area, metabolic activity and living cells compared to control (cisplatin alone), but not significantly more than the corresponding inhibitor alone (Fig. 5A–E). Moreover, we observed a greater effect in terms of decreasing the area of metabolically active cells with the combination of low-dose cisplatin and PI3Kα inhibitors compared with 5 μM cisplatin (Fig. 5E). We found no significant differences following treatment with TGX-221 or AZD8186 in combination with cisplatin compared to cisplatin alone. Differences in the effects observed with the three different assays show that the key combined action of PI3Kα inactivation and cisplatin treatment consists of decreasing cell survival upon tumorosphere dissociation.

Finally, addition of MSCs, which compacted the tumorospheres, tended to decrease the efficiency of PI3Kα inhibitor activity on tumorosphere area, but an effect was always observed (Fig. 6A and B). The absence of a direct effect of all PI3K inhibitors on MSCs was verified (Suppl. Fig. S3).

Compared to cisplatin treatment, treatment with PI3Kα inhibitors results in a decrease in tumorosphere survival, possibly via dissociation of the tumour cell aggregate.

DISCUSSION

Because late diagnosis is common, ovarian cancers associated with peritoneal carcinomatosis frequently develop ascites. This metastatic process involves a transcoelomic migration step requiring tumour cell aggregation within the peritoneal cavity. This 3D structure enhances the ability of tumour cells to survive conventional chemotherapies [2,29]. The current therapeutic arsenal lacks treatments targeting the metastatic disease, which represents a major public health issue due to its morbidity and mortality. To date, HIPEC is of therapeutic interest for the treatment of peritoneal carcinomatosis, but its use remains infrequent because of the potential toxicities [30,31]. Our data demonstrate that PI3Kα inhibitors should be added to the therapeutic arsenal.

We found tumour aggregates in the ascites of all the studied patients with ovarian cancer. Surprisingly, patients with a high number of cell aggregates had a better survival than patients with a low number (Fig. 1A–C). These clinical observations reinforce the need to better understand the formation of ovarian tumour cell aggregates. In this study, we developed a 3D culture method to better mimic the aggregate formation observed within the ascites fluid and responsible for the rapid development of peritoneal carcinomatosis.

PI3K, and more particularly the α isoform, plays a role in the rearrangement of the actin cytoskeleton [14,32]. Actin involvement in migration and invasion well established and, according to our hypothesis, PI3Kα activity would facilitate formation of ovarian tumour cell aggregates [16,17]. To validate this hypothesis, we treated SKOV-3 cell tumorospheres during seeding with different concentrations of the PI3Kα inhibitors A66 [22] and BYL719 [23]. After treatment of these aggregates, and regardless of concentration used, microscopy revealed sphere disorganization, and complete disintegration was seen following treatment with 10 μM of BYL719. While treatment with 10 μM of BYL719 during cell seeding caused a total reduction in measurable sphere area after 7 days, the same treatment started one day later resulted in a 68.5%

reduction in sphere area. This treatment efficacy reduction could be due to a lack of treatment penetration within the spheres [33]. PI3Kα seems to play a role in both formation and maintenance of ovarian tumour cell aggregates.

It has been repeatedly demonstrated that 2D cytotoxicity studies do not account for complete tissue physiology and overestimate the cytotoxic potential of tested molecules [8,34]. In a 3D culture, these cells are 18, 15 or 58 times more resistant to cisplatin at 25, 50 and 100 µM, respectively [8]. In addition, proliferation within the spheres decreases in comparison with cells cultured in 2D, partially explaining why these cells can survive therapies that induce death in replicating cells [8,35]. Here, SKOV-3 cells cultured in 3D show a 33.4% increase in resistance to treatment with 10 µM of BYL719 compared to a 2D culture. Resistance to cisplatin, a standard treatment in HIPEC for ovarian cancer, increased by approximately 70% in this 3D culture (Fig. 4). Inhibitors seem to maintain a concentration-dependent effect at day 4 compared to cisplatin, which at this stage is ineffective (Suppl. Fig. S2A and B), suggesting that inhibitors retain an earlier action on tumorosphere cohesion compared with cisplatin. Whatever the timing of treatment, cisplatin has a significant effect only at a high concentration of 5 µM (Fig. 2I and 3H). At a low concentration of 0.1 µM, BYL719 leads to a significant reduction in the tumorosphere area (Fig. 3D), which suggests it could have an effect on peritoneal carcinomatosis while maintaining low toxicity.

Our hypothesis that PI3Kα acts on spheroid development seems to be verified by the results of our study. PI3Kα action on the actin cytoskeleton could be the source of this effect on spheroids [36]. This hypothesis is reinforced by the knowledge of an existing link between polymerized actin and adhesive molecules such as E- or P-cadherins. P-cadherin expression promotes migratory potential and aggregation of circulating ovarian cancer cells into multicellular aggregates [37]. These elements highlighting the role of actin could in part explain PI3Kα involvement in cell clustering [38,39]. Therapies targeting adhesion between cancer cells of the

same type, such as PI3Kα inhibitors, are worthy of consideration for improving management of peritoneal carcinomatosis. Tumour aggregate disorganization induced by PI3Kα inhibitors would allow a better cisplatin bioavailability within the tumorospheres, by breaking the decreasing diffusion gradient from the periphery to the centre of these 3D structures [40]. Another hypothesis for increased efficiency of cisplatin upon PI3Kα inactivation could be that tumorosphere dissociation decreases the solid stress that builds up in 3D culture [41] and with increased liquid pressure [42] or shear stress caused by ascites fluid motion in the peritoneal cavity [5], or the tensile stress caused by MSCs, increasing the tumor cell's proliferation rate and allowing cisplatin to function. This remains to be demonstrated in follow-up studies.

One parameter that we find key to patient prognosis is the size of tumour aggregates. This could account for the varied response of patients to chemotherapeutic agents. Others have also reported that forming spheroids of small size is more representative of patient's disease [43]. If compression, interstitial pressure and tension increase invasion features through epithelial-to-mesenchymal transition [41,42], our clinical data demonstrate that less aggressive cells tend to grow into larger multicellular aggregates, which could decrease their proliferation rate and increase their death ratio. Others found that the morphology of human donor ascites aggregates was conserved in tumour-bearing mice that had received intraperitoneal injections of these cells [26]. Finding a molecular determinant of such behaviour is of interest to understand the progression of ovarian cancer.

In conclusion, our results show that isolated cells obtained from small tumour aggregates can be treated with PI3Kα inhibitors. This is all the more important given that we find that patients with smaller aggregates have a poorer prognosis. The use of an intraperitoneal PI3Kα inhibitor pretreatment separating aggregates into individual cells allows sensitization of tumorospheres to the treatments used in HIPEC and constitutes a promising alternative to improve the management of a pathology with a very poor prognosis.

Acknowledgements

We thank all members of SigDYN for their comments during the writing of the manuscript, the CRCT core technology platform, particularly Laetitia Ligat, for imaging and Marie Veronique Joubert for her help in MSC culture. JGG's laboratory is part of TOUCAN (Laboratoire d'Excellence, ANR), an integrated research programme on signal-targeted drug resistance. For this topic, JGG's laboratory received funding from the ARC (Foundation for Cancer Research) (PJA20171206596), TOUCAN (Laboratoire d'Excellence, ANR), Fondation de France (BT's salary), and Hôpitaux de Toulouse (AT's salary). The manuscript has been revised for the English by an independent scientific language editing service (Angloscribe).

Author contribution

Adrien Thole: data curation; formal analysis; investigation; methodology; visualization; writing – original draft; review & editing. **Benoît Thibault:** conceptualization; data curation; formal analysis; investigation; methodology; validation; visualization; writing – review & editing. **Céline Basset:** data curation; formal analysis; methodology; resources; visualization; writing – review & editing. **Julie Guillermet-Guibert:** conceptualization; data curation; formal analysis; funding acquisition; investigation; methodology; project administration; supervision; validation; visualization; writing – original draft; writing – review & editing.

Conflict of interest

The authors have no conflict of interest to declare.

References

[1] A. Jemal, F. Bray, M.M. Center, J. Ferlay, E. Ward, D. Forman, Global cancer statistics, CA. Cancer J. Clin. 61 (2011) 69–90. https://doi.org/10.3322/caac.20107.

[2] D.S.P. Tan, R. Agarwal, S.B. Kaye, Mechanisms of transcoelomic metastasis in ovarian cancer, Lancet Oncol. 7 (2006) 925–934. https://doi.org/10.1016/S1470-2045(06)70939-1.

[3] K. Cerne, B. Kobal, Ascites in Advanced Ovarian Cancer, in: O. Devaja, A. Papadopoulos (Eds.), Ovarian Cancer - Pathog. Treat., InTech, 2018. https://doi.org/10.5772/intechopen.72698.

[4] E. Lengyel, Ovarian Cancer Development and Metastasis, Am. J. Pathol. 177 (2010) 1053–1064. https://doi.org/10.2353/ajpath.2010.100105.

[5] I. Rizvi, U.A. Gurkan, S. Tasoglu, N. Alagic, J.P. Celli, L.B. Mensah, Z. Mai, U. Demirci, T. Hasan, Flow induces epithelial-mesenchymal transition, cellular heterogeneity and biomarker modulation in 3D ovarian cancer nodules, Proc. Natl. Acad. Sci. 110 (2013) E1974–E1983. https://doi.org/10.1073/pnas.1216989110.

[6] A.A. Wright, A. Cronin, D.E. Milne, M.A. Bookman, R.A. Burger, D.E. Cohn, M.C. Cristea, J.J. Griggs, N.L. Keating, C.F. Levenback, G. Mantia-Smaldone, U.A. Matulonis, L.A. Meyer, J.C. Niland, J.C. Weeks, D.M. O'Malley, Use and Effectiveness of Intraperitoneal Chemotherapy for Treatment of Ovarian Cancer, J. Clin. Oncol. 33 (2015) 2841–2847. https://doi.org/10.1200/JCO.2015.61.4776.

[7] S. Mabuchi, H. Kuroda, R. Takahashi, T. Sasano, The PI3K/AKT/mTOR pathway as a therapeutic target in ovarian cancer, Gynecol. Oncol. 137 (2015) 173–179. https://doi.org/10.1016/j.ygyno.2015.02.003.

[8] H. Kobayashi, S. Man, C.H. Graham, S.J. Kapitain, B.A. Teicher, R.S. Kerbel, Acquired multicellular-mediated resistance to alkylating agents in cancer, Proc. Natl. Acad. Sci. U. S. A. 90 (1993) 3294–3298.

[9] N. Aceto, A. Bardia, D.T. Miyamoto, M.C. Donaldson, B.S. Wittner, J.A. Spencer, M. Yu, A. Pely, A. Engstrom, H. Zhu, B.W. Brannigan, R. Kapur, S.L. Stott, T. Shioda, S. Ramaswamy, D.T. Ting, C.P. Lin, M. Toner, D.A. Haber, S. Maheswaran, Circulating tumor cell clusters are oligoclonal precursors of breast cancer metastasis, Cell. 158 (2014) 1110–1122. https://doi.org/10.1016/j.cell.2014.07.013.

[10] M. Castells, B. Thibault, J.-P. Delord, B. Couderc, Implication of Tumor Microenvironment in Chemoresistance: Tumor-Associated Stromal Cells Protect Tumor Cells from Cell Death, Int. J. Mol. Sci. 13 (2012) 9545–9571. https://doi.org/10.3390/ijms13089545.

[11] J.M.L. Roodhart, L.G.M. Daenen, E.C.A. Stigter, H.-J. Prins, J. Gerrits, J.M. Houthuijzen, M.G. Gerritsen, H.S. Schipper, M.J.G. Backer, M. van Amersfoort, J.S.P. Vermaat, P. Moerer, K. Ishihara, E. Kalkhoven, J.H. Beijnen, P.W.B. Derksen, R.H. Medema, A.C. Martens, A.B. Brenkman, E.E. Voest, Mesenchymal Stem Cells Induce Resistance to Chemotherapy through the Release of Platinum-Induced Fatty Acids, Cancer Cell. 20 (2011) 370–383. https://doi.org/10.1016/j.ccr.2011.08.010.

[12] J.-H. Lee, S.-K. Kim, I.A. Khawar, S.-Y. Jeong, S. Chung, H.-J. Kuh, Microfluidic co-culture of pancreatic tumor spheroids with stellate cells as a novel 3D model for investigation of stroma-mediated cell motility and drug resistance, J. Exp. Clin. Cancer Res. 37 (2018). https://doi.org/10.1186/s13046-017-0654-6.

[13] A. Kabashima-Niibe, H. Higuchi, H. Takaishi, Y. Masugi, Y. Matsuzaki, Y. Mabuchi, S. Funakoshi, M. Adachi, Y. Hamamoto, S. Kawachi, K. Aiura, Y. Kitagawa, M. Sakamoto, T. Hibi, Mesenchymal stem cells regulate epithelial-mesenchymal transition and tumor progression of pancreatic cancer cells, Cancer Sci. 104 (2013) 157–164. https://doi.org/10.1111/cas.12059.

[14] R. Baer, C. Cintas, M. Dufresne, S. Cassant-Sourdy, N. Schönhuber, L. Planque, H. Lulka, B. Couderc, C. Bousquet, B. Garmy-Susini, B. Vanhaesebroeck, S. Pyronnet, D. Saur, J. Guillermet-Guibert, Pancreatic cell plasticity and cancer initiation induced by oncogenic Kras is completely dependent on wild-type PI 3-kinase p110α, Genes Dev. 28 (2014) 2621–2635. https://doi.org/10.1101/gad.249409.114.

[15] Y. Zhang, P. Kwok-Shing Ng, M. Kucherlapati, F. Chen, Y. Liu, Y.H. Tsang, G. de Velasco, K.J. Jeong, R. Akbani, A. Hadjipanayis, A. Pantazi, C.A. Bristow, E. Lee, H.S. Mahadeshwar, J.

Tang, J. Zhang, L. Yang, S. Seth, S. Lee, X. Ren, X. Song, H. Sun, J. Seidman, L.J. Luquette, R. Xi, L. Chin, A. Protopopov, T.F. Westbrook, C.S. Shelley, T.K. Choueiri, M. Ittmann, C. Van Waes, J.N. Weinstein, H. Liang, E.P. Henske, A.K. Godwin, P.J. Park, R. Kucherlapati, K.L. Scott, G.B. Mills, D.J. Kwiatkowski, C.J. Creighton, A Pan-Cancer Proteogenomic Atlas of PI3K/AKT/mTOR Pathway Alterations, Cancer Cell. 31 (2017) 820–832.e3. https://doi.org/10.1016/j.ccell.2017.04.013.

[16] B. Vanhaesebroeck, J. Guillermet-Guibert, M. Graupera, B. Bilanges, The emerging mechanisms of isoform-specific PI3K signalling, Nat. Rev. Mol. Cell Biol. 11 (2010) 329–341. https://doi.org/10.1038/nrm2882.

[17] K. Tsujita, T. Itoh, Phosphoinositides in the regulation of actin cortex and cell migration, Biochim. Biophys. Acta. 1851 (2015) 824–831. https://doi.org/10.1016/j.bbalip.2014.10.011.

[18] H. Bai, H. Li, W. Li, T. Gui, J. Yang, D. Cao, K. Shen, The PI3K/AKT/mTOR pathway is a potential predictor of distinct invasive and migratory capacities in human ovarian cancer cell lines, Oncotarget. 6 (2015). https://doi.org/10.18632/oncotarget.4550.

[19] D.A. Levine, Frequent Mutation of the PIK3CA Gene in Ovarian and Breast Cancers, Clin. Cancer Res. 11 (2005) 2875–2878. https://doi.org/10.1158/1078-0432.CCR-04-2142.

[20] I.A. Mayer, V.G. Abramson, L. Formisano, J.M. Balko, M.V. Estrada, M.E. Sanders, D. Juric, D. Solit, M.F. Berger, H.H. Won, Y. Li, L.C. Cantley, E. Winer, C.L. Arteaga, A Phase Ib Study of Alpelisib (BYL719), a PI3Kα-Specific Inhibitor, with Letrozole in ER $^{+}$ /HER2 $^{-}$ Metastatic Breast Cancer, Clin. Cancer Res. 23 (2017) 26–34. https://doi.org/10.1158/1078-0432.CCR-16-0134.

[21] F. André, E. Ciruelos, G. Rubovszky, M. Campone, S. Loibl, H.S. Rugo, H. Iwata, P. Conte, I.A. Mayer, B. Kaufman, T. Yamashita, Y.-S. Lu, K. Inoue, M. Takahashi, Z. Pápai, A.-S. Longin, D. Mills, C. Wilke, S. Hirawat, D. Juric, Alpelisib for *PIK3CA* -Mutated, Hormone Receptor–Positive Advanced Breast Cancer, N. Engl. J. Med. 380 (2019) 1929–1940. https://doi.org/10.1056/NEJMoa1813904.

[22] S. Jamieson, J.U. Flanagan, S. Kolekar, C. Buchanan, J.D. Kendall, W.-J. Lee, G.W. Rewcastle, W.A. Denny, R. Singh, J. Dickson, B.C. Baguley, P.R. Shepherd, A drug targeting only p110α can block phosphoinositide 3-kinase signalling and tumour growth in certain cell types, Biochem. J. 438 (2011) 53–62. https://doi.org/10.1042/BJ20110502.

[23] C. Fritsch, A. Huang, C. Chatenay-Rivauday, C. Schnell, A. Reddy, M. Liu, A. Kauffmann, D. Guthy, D. Erdmann, A. De Pover, P. Furet, H. Gao, S. Ferretti, Y. Wang, J. Trappe, S.M. Brachmann, S.-M. Maira, C. Wilson, M. Boehm, C. Garcia-Echeverria, P. Chene, M. Wiesmann, R. Cozens, J. Lehar, R. Schlegel, G. Caravatti, F. Hofmann, W.R. Sellers, Characterization of the Novel and Specific PI3K Inhibitor NVP-BYL719 and Development of the Patient Stratification Strategy for Clinical Trials, Mol. Cancer Ther. 13 (2014) 1117–1129. https://doi.org/10.1158/1535-7163.MCT-13-0865.

[24] S.P. Jackson, S.M. Schoenwaelder, I. Goncalves, W.S. Nesbitt, C.L. Yap, C.E. Wright, V. Kenche, K.E. Anderson, S.M. Dopheide, Y. Yuan, S.A. Sturgeon, H. Prabaharan, P.E. Thompson, G.D. Smith, P.R. Shepherd, N. Daniele, S. Kulkarni, B. Abbott, D. Saylik, C. Jones, L. Lu, S. Giuliano, S.C. Hughan, J.A. Angus, A.D. Robertson, H.H. Salem, PI 3-kinase p110β: a new target for antithrombotic therapy, Nat. Med. 11 (2005) 507–514. https://doi.org/10.1038/nm1232.

[25] B. Barlaam, S. Cosulich, S. Degorce, M. Fitzek, S. Green, U. Hancox, C. Lambert-van der Brempt, J.-J. Lohmann, M. Maudet, R. Morgentin, M.-J. Pasquet, A. Péru, P. Plé, T. Saleh, M. Vautier, M. Walker, L. Ward, N. Warin, Discovery of (R)-8-(1-(3,5-Difluorophenylamino)ethyl)-N , N -dimethyl-2-morpholino-4-oxo-4 H -chromene-6-carboxamide (AZD8186): A Potent and Selective Inhibitor of PI3Kβ and PI3Kδ for the Treatment of PTEN-Deficient Cancers, J. Med. Chem. 58 (2015) 943–962. https://doi.org/10.1021/jm501629p.

[26] A. Latifi, R.B. Luwor, M. Bilandzic, S. Nazaretian, K. Stenvers, J. Pyman, H. Zhu, E.W. Thompson, M.A. Quinn, J.K. Findlay, N. Ahmed, Isolation and Characterization of Tumor Cells from the Ascites of Ovarian Cancer Patients: Molecular Phenotype of Chemoresistant Ovarian Tumors, PLoS ONE. 7 (2012) e46858. https://doi.org/10.1371/journal.pone.0046858.

[27] E. Pons-Tostivint, B. Thibault, J. Guillermet-Guibert, Targeting PI3K Signaling in Combination Cancer Therapy, Trends Cancer. 3 (2017) 454–469. https://doi.org/10.1016/j.trecan.2017.04.002.
[28] S. Ohie, Y. Udagawa, A. Kozu, Y. Komuro, D. Aoki, S. Nozawa, A.R. Moossa, R.M. Hoffman, Cisplatin sensitivity of ovarian cancer in the histoculture drug response assay correlates to clinical response to combination chemotherapy with cisplatin, doxorubicin and cyclophosphamide, Anticancer Res. 20 (2000) 2049–2054.
[29] J. Liao, F. Qian, N. Tchabo, P. Mhawech-Fauceglia, A. Beck, Z. Qian, X. Wang, W.J. Huss, S.B. Lele, C.D. Morrison, K. Odunsi, Ovarian Cancer Spheroid Cells with Stem Cell-Like Properties Contribute to Tumor Generation, Metastasis and Chemotherapy Resistance through Hypoxia-Resistant Metabolism, PLoS ONE. 9 (2014) e84941. https://doi.org/10.1371/journal.pone.0084941.
[30] D. Goéré, D. Malka, D. Tzanis, V. Gava, V. Boige, C. Eveno, L. Maggiori, F. Dumont, M. Ducreux, D. Elias, Is there a possibility of a cure in patients with colorectal peritoneal carcinomatosis amenable to complete cytoreductive surgery and intraperitoneal chemotherapy?, Ann. Surg. 257 (2013) 1065–1071. https://doi.org/10.1097/SLA.0b013e31827e9289.
[31] W.J. van Driel, S.N. Koole, K. Sikorska, J.H. Schagen van Leeuwen, H.W.R. Schreuder, R.H.M. Hermans, I.H.J.T. de Hingh, J. van der Velden, H.J. Arts, L.F.A.G. Massuger, A.G.J. Aalbers, V.J. Verwaal, J.M. Kieffer, K.K. Van de Vijver, H. van Tinteren, N.K. Aaronson, G.S. Sonke, Hyperthermic Intraperitoneal Chemotherapy in Ovarian Cancer, N. Engl. J. Med. 378 (2018) 230–240. https://doi.org/10.1056/NEJMoa1708618.
[32] C.C. Campa, E. Ciraolo, A. Ghigo, G. Germena, E. Hirsch, Crossroads of PI3K and Rac pathways, Small GTPases. 6 (2015) 71–80. https://doi.org/10.4161/21541248.2014.989789.
[33] J.M. Ayuso, H.A. Basheer, R. Monge, P. Sánchez-Álvarez, M. Doblaré, S.D. Shnyder, V. Vinader, K. Afarinkia, L.J. Fernández, I. Ochoa, Study of the Chemotactic Response of Multicellular Spheroids in a Microfluidic Device, PLOS ONE. 10 (2015) e0139515. https://doi.org/10.1371/journal.pone.0139515.
[34] K. Shield, M.L. Ackland, N. Ahmed, G.E. Rice, Multicellular spheroids in ovarian cancer metastases: Biology and pathology, Gynecol. Oncol. 113 (2009) 143–148. https://doi.org/10.1016/j.ygyno.2008.11.032.
[35] K.M. Burleson, R.C. Casey, K.M. Skubitz, S.E. Pambuccian, T.R. Oegema, A.P.. Skubitz, Ovarian carcinoma ascites spheroids adhere to extracellular matrix components and mesothelial cell monolayers, Gynecol. Oncol. 93 (2004) 170–181. https://doi.org/10.1016/j.ygyno.2003.12.034.
[36] E.C. Lien, C.C. Dibble, A. Toker, PI3K signaling in cancer: beyond AKT, Curr. Opin. Cell Biol. 45 (2017) 62–71. https://doi.org/10.1016/j.ceb.2017.02.007.
[37] A. Usui, S.Y. Ko, N. Barengo, H. Naora, P-Cadherin Promotes Ovarian Cancer Dissemination Through Tumor Cell Aggregation and Tumor–Peritoneum Interactions, Mol. Cancer Res. 12 (2014) 504–513. https://doi.org/10.1158/1541-7786.MCR-13-0489.
[38] L. Saias, A. Gomes, M. Cazales, B. Ducommun, V. Lobjois, Cell-Cell Adhesion and Cytoskeleton Tension Oppose Each Other in Regulating Tumor Cell Aggregation, Cancer Res. 75 (2015) 2426–2433. https://doi.org/10.1158/0008-5472.CAN-14-3534.
[39] J.O.A.M. van Baal, C.J.F. van Noorden, R. Nieuwland, K.K. Van de Vijver, A. Sturk, W.J. van Driel, G.G. Kenter, C.A.R. Lok, Development of Peritoneal Carcinomatosis in Epithelial Ovarian Cancer: A Review, J. Histochem. Cytochem. 66 (2018) 67–83. https://doi.org/10.1369/0022155417742897.
[40] S. Sant, P.A. Johnston, The production of 3D tumor spheroids for cancer drug discovery, Drug Discov. Today Technol. 23 (2017) 27–36. https://doi.org/10.1016/j.ddtec.2017.03.002.
[41] M. Delarue, F. Montel, D. Vignjevic, J. Prost, J.-F. Joanny, G. Cappello, Compressive Stress Inhibits Proliferation in Tumor Spheroids through a Volume Limitation, Biophys. J. 107 (2014) 1821–1828. https://doi.org/10.1016/j.bpj.2014.08.031.
[42] Y. Klymenko, R.B. Wates, H. Weiss-Bilka, R. Lombard, Y. Liu, L. Campbell, O. Kim, D. Wagner, M.J. Ravosa, M.S. Stack, Modeling the effect of ascites-induced compression on ovarian cancer multicellular aggregates, Dis. Model. Mech. 11 (2018) dmm034199. https://doi.org/10.1242/dmm.034199.

[43] S. Raghavan, M.R. Ward, K.R. Rowley, R.M. Wold, S. Takayama, R.J. Buckanovich, G. Mehta, Formation of stable small cell number three-dimensional ovarian cancer spheroids using hanging drop arrays for preclinical drug sensitivity assays, Gynecol. Oncol. 138 (2015) 181–189. https://doi.org/10.1016/j.ygyno.2015.04.014.

Figure legends:

Figure 1: Modelling tumour aggregates derived from ovarian cancer ascites. (A) Immunohistochemistry of high-grade ovarian serous carcinoma from ascites fluid, in which tumorospheres are indicated by arrows, (x100 and x400 magnification). PAP = Papanicolaou, MGG = May-Grünwald-Giemsa, PAS = Periodic acid–Schiff. (B) Survival curves from patients with high-grade serous ovarian cancer presenting with aggregate-rich or aggregate-poor ascites; 12 patients. (C) Evolution of tumorosphere morphology 1, 4 or 7 days after seeding. (D) Model of transcoelomic dissemination from the primary tumour facilitated by the flow of liquid and formation of tumorospheres. (E) Morphology and (F) area of SKOV-3-GFP (green fluorescent protein) tumorospheres. Measurements with ZEN® software (x5 magnification, fluorescence, $n \geq 2$). Comparison of the tumorosphere area with 5000 or 10000 SKOV-3-GFP cells on day 14 by Student t-test $p < 0.01$ (**). (G) (left) Evolution of living cell numbers assessed by the alamarBlue™ assay and (right) GFP fluorescence over time in tumorospheres formed of 5000 SKOV-3-GFP cells. (H) Morphology of heterotypic tumorospheres comprising 5000 SKOV-3-GFP cells (green) cultured with or without different numbers of mesenchymal stem cells (MSCs) (5, 50, 500, 5000) 1, 4 or 7 days after seeding.

Figure 2: PI3Kα inhibition prevents formation of ovarian cancer cell tumorospheres. (A) 5,000 SKOV-3-GFP cells that will form tumouropheres at day (d)1 were treated or not at d0 and d4 with A66 and BYL719 (1 and 10 μM) or cisplatin (0.5 and 5 μM). (B) SKOV-3 cells were serum-deprived overnight, pre-treated for 1 h with specific PI3Kα inhibitors and then serum-activated for 15 minutes. Actin-standardized quantification of the amount of (C) phospho-Akt (S473) and (D) phospho-Akt (T308) relative to the control condition (without treatment). (E, F) SKOV-3-GFP tumorospheres were treated according to the schedule in (A) and morphology was observed 1, 4 or 7 days after seeding. (G, H) Area or (I, J) fluorescence intensity were evaluated at d1, d4 and d7 using ZEN® software (x5 magnification), $n \geq 3$, mean +/- SEM (ANOVA test comparison with the control condition of the corresponding observation day, $p < 0.001$ (***), $p < 0.01$ (**), $p < 0.05$ (*)).

Figure 3: PI3Kα selective inhibition prevents maintenance of ovarian cancer cell tumorospheres. (A) Tumorospheres formed of 5,000 SKOV-3-GFP cells were treated or not at d1 and d4 with A66, BYL719, TGX-221 or AZD8186 (0.01, 0.1, 1 and 10 µM) or cisplatin (0.5 and 5 µM). (B and G) Tumorosphere morphology was evaluated on d1, d4 and d7. (C–F and H) Tumorosphere area was evaluated on d1, d4 and d7 using ZEN® software (x5 magnification), n ≥ 3, Mean +/- SEM (ANOVA test comparison with the control condition of the corresponding observation day, p <0.001 (***), p <0.01 (**), p <0.05 (*)).

Figure 4: Only PI3Kα inhibition impacts ovarian tumour cell viability in 3D culture. (A) Tumorospheres formed of 5,000 SKOV-3-GFP cells were treated or not at d1 and d4 with A66, BYL719, TGX-221 or AZD8186 (0.01, 0.1, 1 and 10 µM) or cisplatin (0.5 and 5 µM). Living cell percentages were evaluated on d7 by (B, C) the MTT test and the (D, E) alamarBlue™ test (3D), n ≥ 3. (F) Tumorosphere morphology was evaluated on d7 using ZEN® software (in fluorescence, x5 magnification); living cells were labelled with calcein (white), n ≥ 3. (G and H) The area of living cells after treatment was quantified using ImageJ® software, n = 2. Mean +/- SEM (ANOVA test comparison with the control condition of the corresponding observation day, p <0.001 (***), p <0.01 (**), p <0.05 (*)).

Figure 5: PI3K inhibitors sensitize 3D cultured cells to the antitumoural effect of low-concentration cisplatin. Tumoursospheres formed of 5,000 SKOV-3 cells were treated or not on d1 and d4 after seeding with a fixed concentration of 1 µM of A66, BYL719, TGX-221, or AZD8186, in combination or not with increasing concentrations of cisplatin (0.05, 0.5, 5 µM). (A) Tumorosphere morphology and (C) area (n ≥ 3) were evaluated using ZEN® software (in fluorescence, x5 magnification). (D) Living cell percentages were evaluated on day 7 by the alamarBlue™ test (n ≥ 3). (B) Living cells were marked with calcein and (E) the living cell area after treatment was quantified using ImageJ® software (n = 2), mean +/- SEM (ANOVA test comparison with cisplatin

concentration and the control of the corresponding observation day, $p < 0.001$ (***), $p < 0.01$ (**), $p < 0.05$ (*)).

Figure 6: PI3Kα inhibitors remain efficient in tumorospheres compacted by mesenchymal stem cells. Tumorospheres formed of 5,000 SKOV-3-GFP cells (green) associated with different ratios of MSCs (labelled in red using Quantum Dots) were produced and treated with 1 or 10 µM of A66 or BYL719. (A) Tumorosphere morphology and (B) area (n = 3) were evaluated using ZEN® software (in fluorescence, x5 magnification) on d7. Mean +/- SEM

Graphical abstract: Schematic representation of PI3Kα involvement in tumour cell aggregates from ascites. 1) Known involvement of PI3Kα in ovarian primary tumours. 2) PI3Kα participates in tumorosphere formation within the peritoneum (treatment with PI3Kα inhibitors causes a delay in the formation of clusters). 3) PI3Kα participates in the maintenance of tumorospheres and in resistance to conventional treatment of peritoneal carcinomatosis. PI3Kα is a target to prevent transcoelomic dissemination and maintenance of tumorospheres in patients with ovarian cancer.

Supplementary Figure S1: Development of heterotypic tumorospheres. (A) Area and (B) morphology of MSC tumorospheres. Measurements with ZEN® software (x5 magnification, $n \geq 2$). (C) Observation of the formation of fibrous-like structures within MSC aggregates. 5000 SKOV-3-GFP cells associated with different MSC ratios (5, 50, 500 or 5000) were seeded and (D) area and (E) GFP fluorescence intensity were evaluated at d1, d4 and d7 using ZEN® software (in fluorescence, x5 magnification, n = 3). (F) Observation of heterotypic tumorospheres of SKOV-3 cells (green) and MSCs (red). Mean +/- SEM (ANOVA test comparison with the condition without MSCs at the corresponding observation day, $p < 0.001$ (***), $p < 0.01$ (**), $p < 0.05$ (*)).

Supplementary Figure S2: Effects of PI3K inhibitors and cisplatin on SKOV-3 tumorospheres. Tumorospheres formed of 5000 SKOV-3 cells were produced and treated or not with A66, BYL719, TGX-221, AZD8186 or cisplatin 24 h after seeding. (A, B) Living cell percentages were evaluated on d4 by the alamarBlue™ test. (C) Living cells were labelled with calcein (green) and dead cells with EthD-1 (red) using the LIVE/DEAD® kit. Mean +/- SEM (n = 3).

Supplementary Figure S3: MSC tumorospheres treated with PI3K inhibitors or cisplatin. Tumorospheres formed of 5000 MSCs were produced and treated or not with A66, BYL719, or cisplatin 24 h after seeding. (A, B) Morphology and (C, D) area of MSC tumorospheres were measured using ZEN® software (x5 magnification, n = 3).

Supplementary Table S1: Patient data. Data corresponding to the ascites samples isolated from patients. Patient number, age (in years), histology, aggregate numbers (per microscopy field) and white blood cell numbers (per mm^3) are represented. The ascites dilution used to determine the aggregate numbers was normalized to the white blood cell number. A normalized aggregate number was determined by multiplying these two parameters. Aggregate-rich ascites had a normalized aggregate number above 100,000, while aggregate-poor ascites had a normalized aggregate number below 100,000.

The lipid kinase PI3Kα is required for aggregation and survival of ovarian intraperitoneal cancer cells.

Authors

Thole A [1,2], Thibault B [1,2], Basset C [1,2,3], Guillermet-Guibert J [1,2]*.

Highlights

- The detection of neoplastic cells in malignant serous effusions is a marker of ovarian cancer tumor progression.
- The size of the ascitic tumour aggregates influences positively the prognosis of the patients.
- PI3Kα, which gene is highly mutated and amplified in ovarian cancers, induces cell compaction that favors therapy resistance.
- The clinically approved therapies that target PI3Kα decreased the survival of ovarian cancer cells from ascites.
- Dissociation of the tumour aggregates leads to an increased sensitivity to cisplatin therapies.

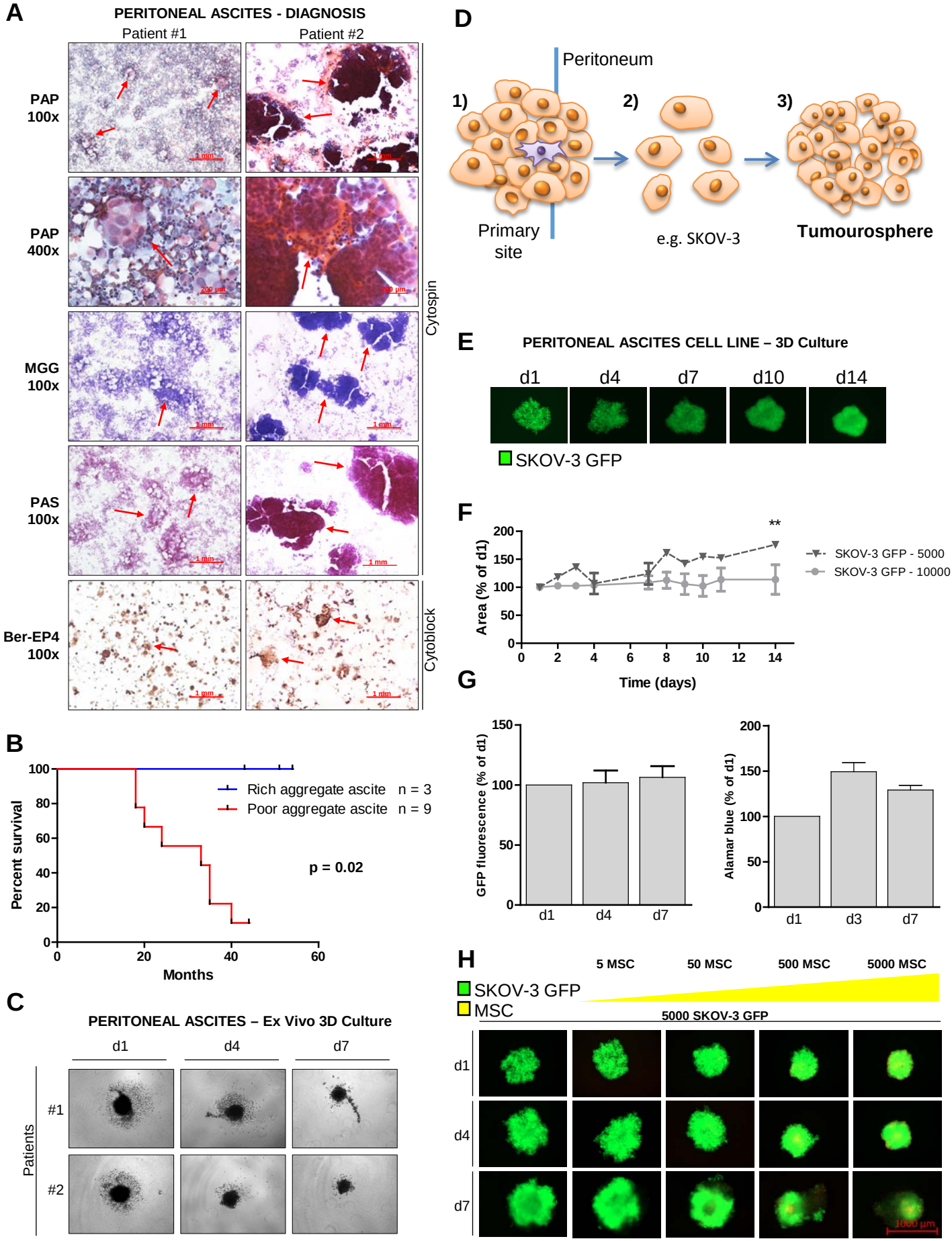
A
PERITONEAL ASCITES - DIAGNOSIS
Patient #1
Patient #2
PAP 100x
PAP 400x
MGG 100x
PAS 100x
Ber-EP4 100x
Cytospin
Cytoblock
B
Percent survival
Months
Rich aggregate ascite n = 3
Poor aggregate ascite n = 9
p = 0.02
C
PERITONEAL ASCITES – Ex Vivo 3D Culture
d1
d4
d7
Patients
#1
#2
D
Peritoneum
1)
2)
3)
Primary site
e.g. SKOV-3
Tumourosphere
E
PERITONEAL ASCITES CELL LINE – 3D Culture
d1
d4
d7
d10
d14
SKOV-3 GFP
F
Area (% of d1)
Time (days)
SKOV-3 GFP - 5000
SKOV-3 GFP - 10000
**
G
GFP fluorescence (% of d1)
Alamar blue (% of d1)
d1
d4
d7
d3
H
5 MSC
50 MSC
500 MSC
5000 MSC
SKOV-3 GFP
MSC
5000 SKOV-3 GFP
d1
d4
d7

Figure 1

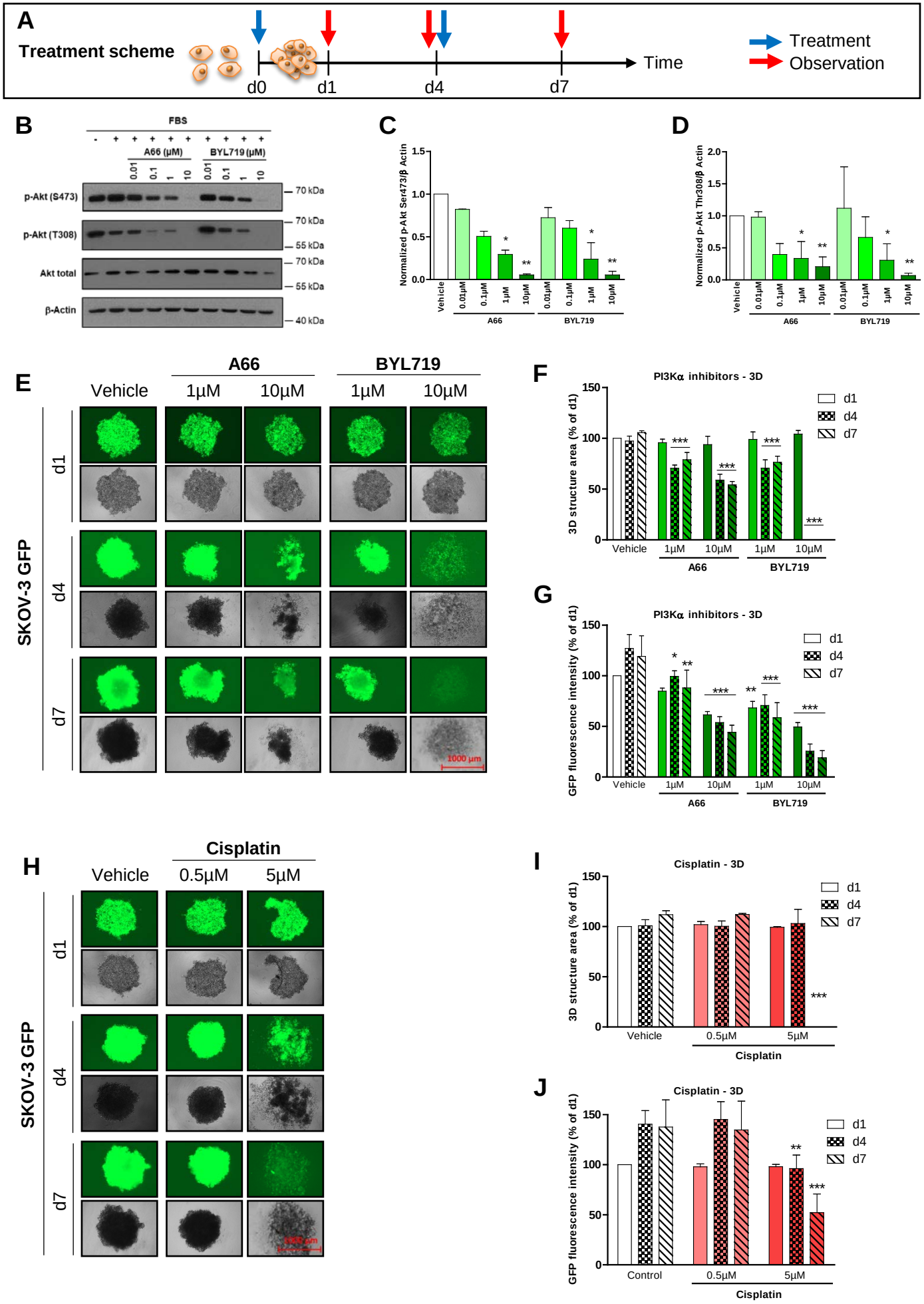
A
Treatment scheme
d0
d1
d4
d7
Time
Treatment
Observation
B
FBS
A66 (μM)
BYL719 (μM)
0.01
0.1
1
10
p-Akt (S473)
p-Akt (T308)
Akt total
β-Actin
70 kDa
55 kDa
40 kDa
C
Normalized p-Akt Ser473/β Actin
Vehicle
A66
BYL719
D
Normalized p-Akt Thr308/β Actin
E
A66
BYL719
Vehicle
1μM
10μM
SKOV-3 GFP
d1
d4
d7
1000 μm
F
PI3Kα inhibitors - 3D
3D structure area (% of d1)
d1
d4
d7
G
GFP fluorescence intensity (% of d1)
H
Cisplatin
0.5μM
5μM
I
Cisplatin - 3D
J
Control

Figure 2

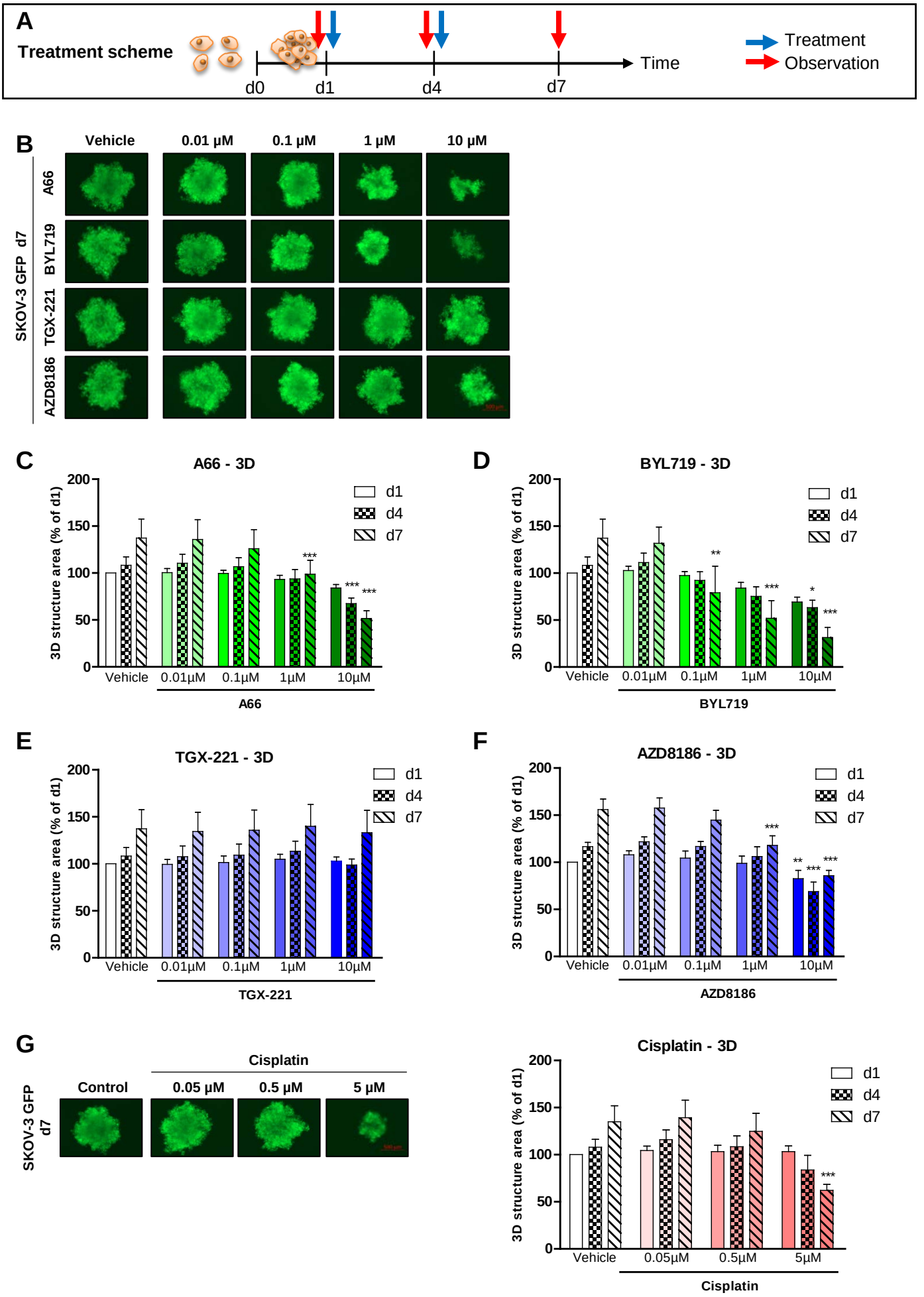
A
Treatment scheme
d0
d1
d4
d7
Time
Treatment
Observation
B
Vehicle
0.01 µM
0.1 µM
1 µM
10 µM
SKOV-3 GFP d7
A66
BYL719
TGX-221
AZD8186
C
A66 - 3D
3D structure area (% of d1)
d1
d4
d7
Vehicle
0.01µM
0.1µM
1µM
10µM
A66
D
BYL719 - 3D
BYL719
E
TGX-221 - 3D
TGX-221
F
AZD8186 - 3D
AZD8186
G
Cisplatin
Control
0.05 µM
0.5 µM
5 µM
SKOV-3 GFP d7
Cisplatin - 3D
0.05µM
0.5µM
5µM

Figure 3

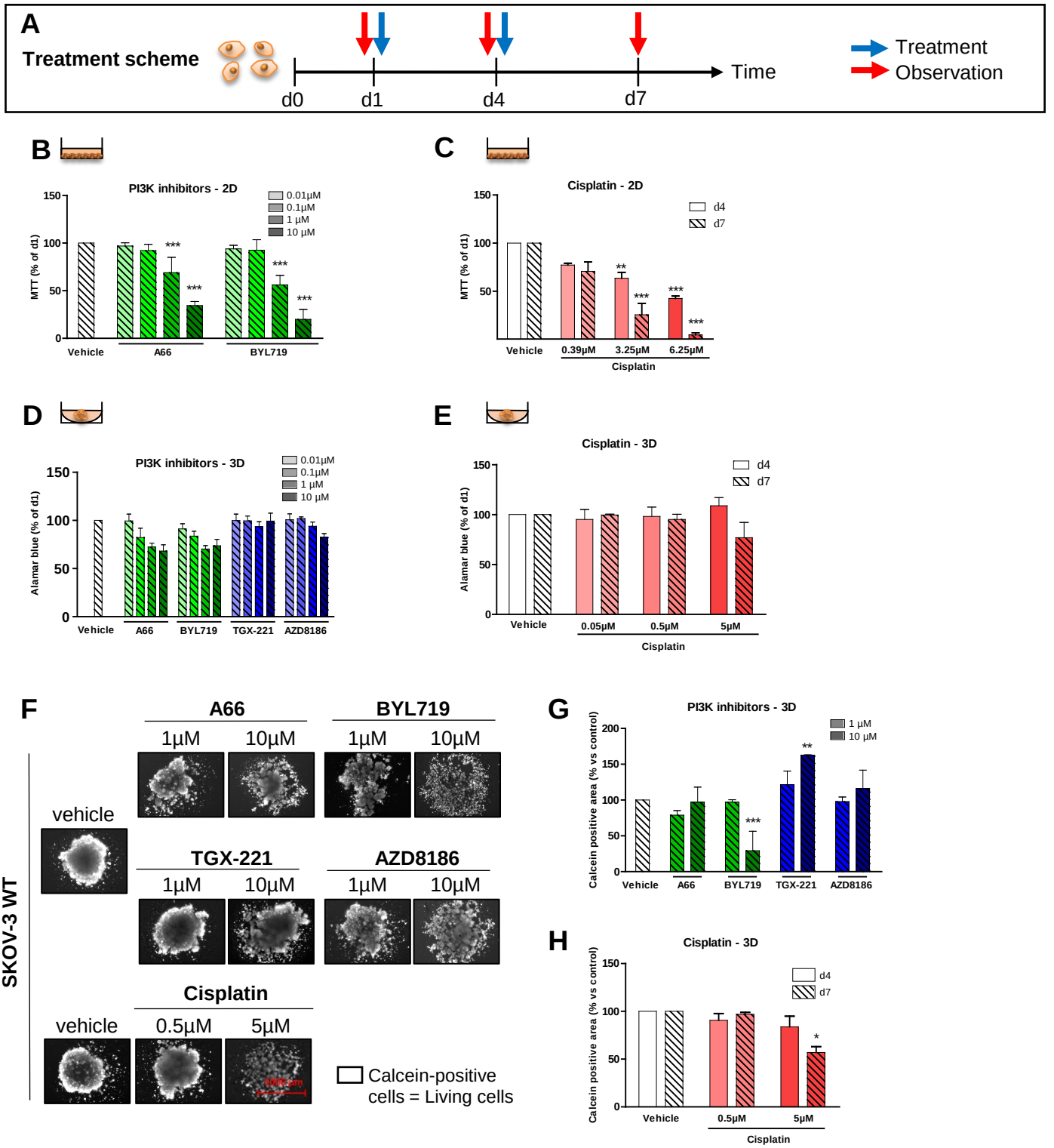
A
Treatment scheme
d0
d1
d4
d7
Time
Treatment
Observation
B
PI3K inhibitors - 2D
0.01µM
0.1µM
1 µM
10 µM
MTT (% of d1)
Vehicle
A66
BYL719
C
Cisplatin - 2D
d4
d7
MTT (% of d1)
Vehicle
0.39µM
3.25µM
6.25µM
Cisplatin
D
PI3K inhibitors - 3D
0.01µM
0.1µM
1 µM
10 µM
Alamar blue (% of d1)
Vehicle
A66
BYL719
TGX-221
AZD8186
E
Cisplatin - 3D
d4
d7
Alamar blue (% of d1)
Vehicle
0.05µM
0.5µM
5µM
Cisplatin
F
SKOV-3 WT
A66
1µM
10µM
BYL719
1µM
10µM
vehicle
TGX-221
1µM
10µM
AZD8186
1µM
10µM
Cisplatin
vehicle
0.5µM
5µM
Calcein-positive cells = Living cells
G
PI3K inhibitors - 3D
1 µM
10 µM
Calcein positive area (% vs control)
Vehicle
A66
BYL719
TGX-221
AZD8186
H
Cisplatin - 3D
d4
d7
Calcein positive area (% vs control)
Vehicle
0.5µM
5µM
Cisplatin

Figure 4

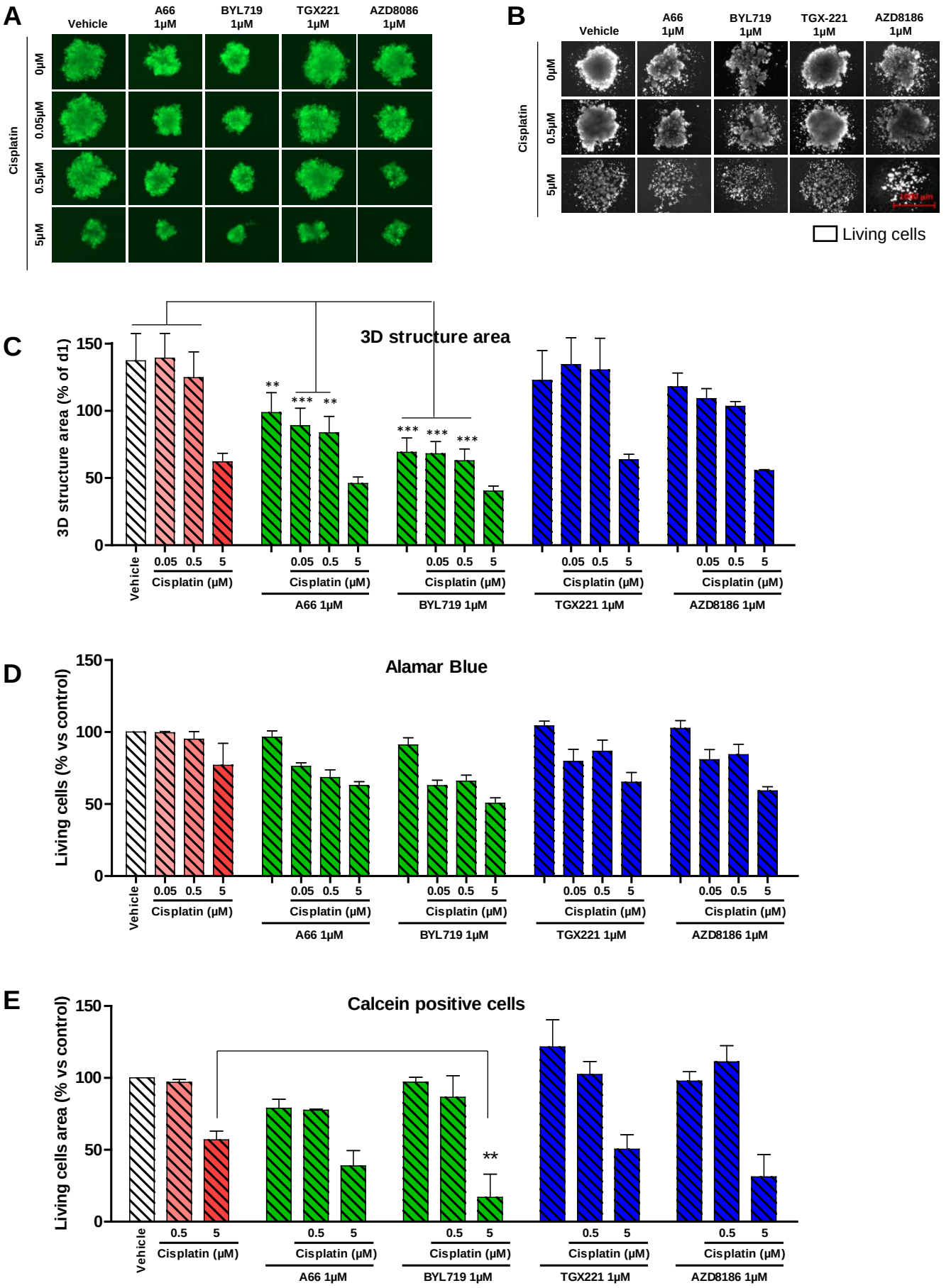
A
Vehicle
A66 1µM
BYL719 1µM
TGX221 1µM
AZD8086 1µM
Cisplatin
0µM
0.05µM
0.5µM
5µM
B
Vehicle
A66 1µM
BYL719 1µM
TGX-221 1µM
AZD8186 1µM
Cisplatin
0µM
0.5µM
5µM
Living cells
C
3D structure area
3D structure area (% of d1)
150
100
50
0
Vehicle
0.05 0.5 5
Cisplatin (µM)
A66 1µM
BYL719 1µM
TGX221 1µM
AZD8186 1µM
D
Alamar Blue
Living cells (% vs control)
E
Calcein positive cells
Living cells area (% vs control)
0.5 5

Figure 5

A

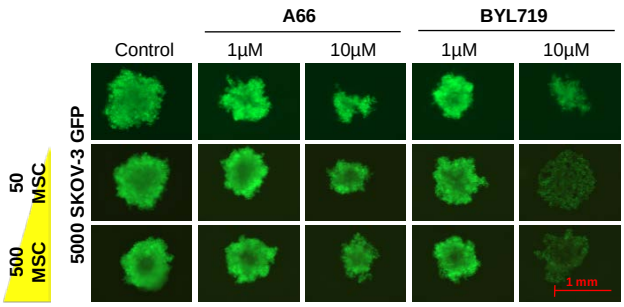
A66
BYL719
Control
1µM
10µM
1µM
10µM
5000 SKOV-3 GFP
50 MSC
500 MSC
1 mm

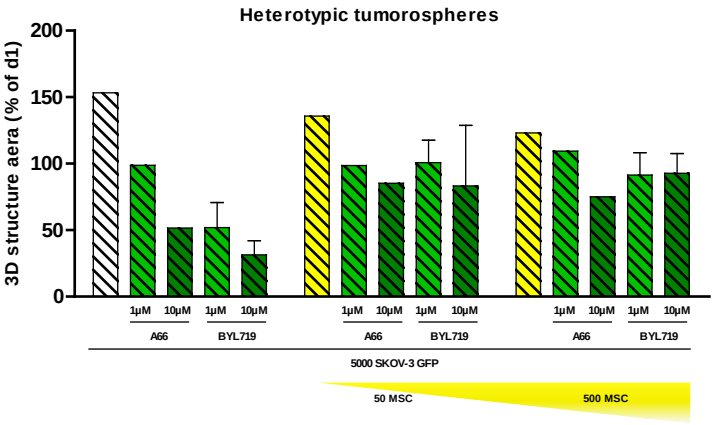
Heterotypic tumorospheres
3D structure aera (% of d1)
200
150
100
50
0
1µM
10µM
1µM
10µM
A66
BYL719
5000 SKOV-3 GFP
50 MSC
500 MSC

Figure 6

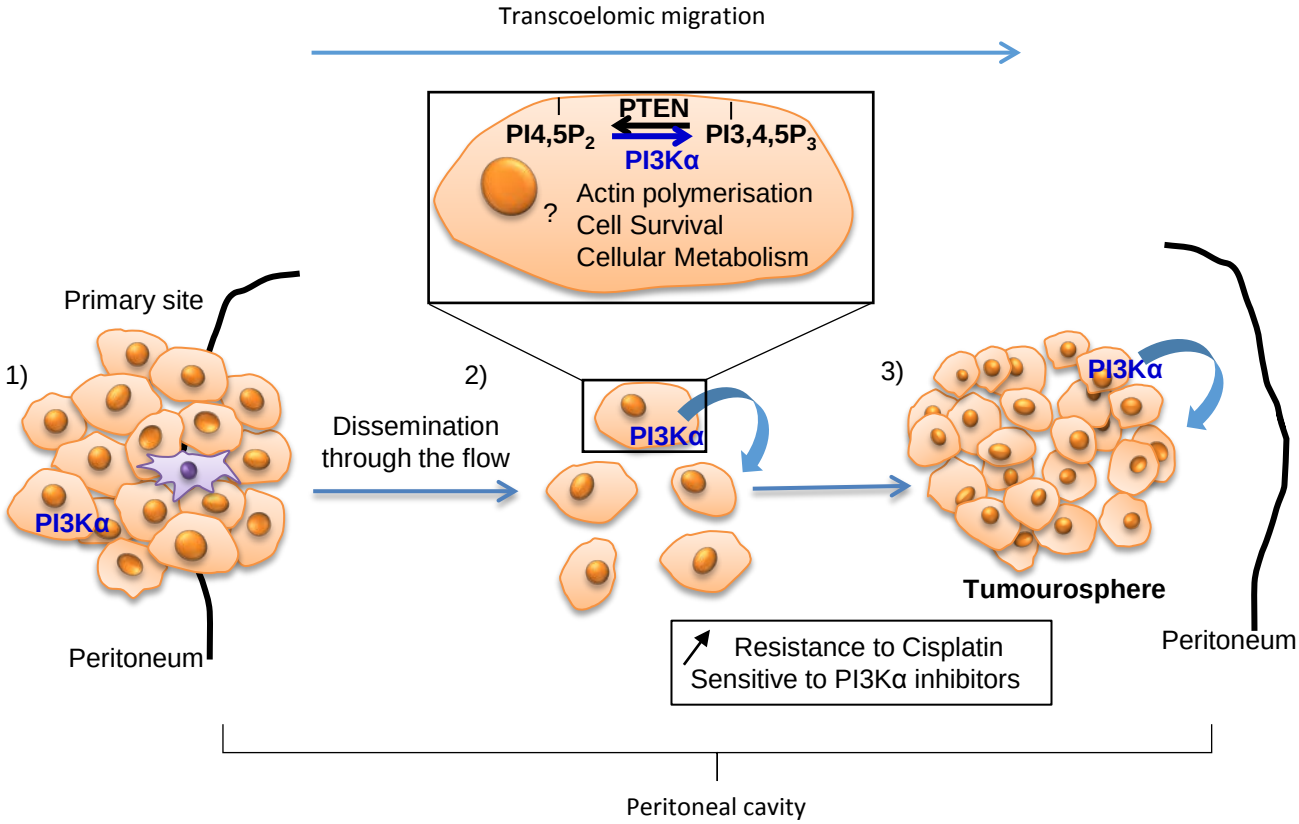
Transcoelomic migration
PTEN
PI4,5P2
PI3,4,5P3
PI3Kα
?
Actin polymerisation
Cell Survival
Cellular Metabolism
Primary site
1)
PI3Kα
Peritoneum
Dissemination
through the flow
2)
PI3Kα
3)
PI3Kα
Tumourosphere
Resistance to Cisplatin
Sensitive to PI3Kα inhibitors
Peritoneum
Peritoneal cavity

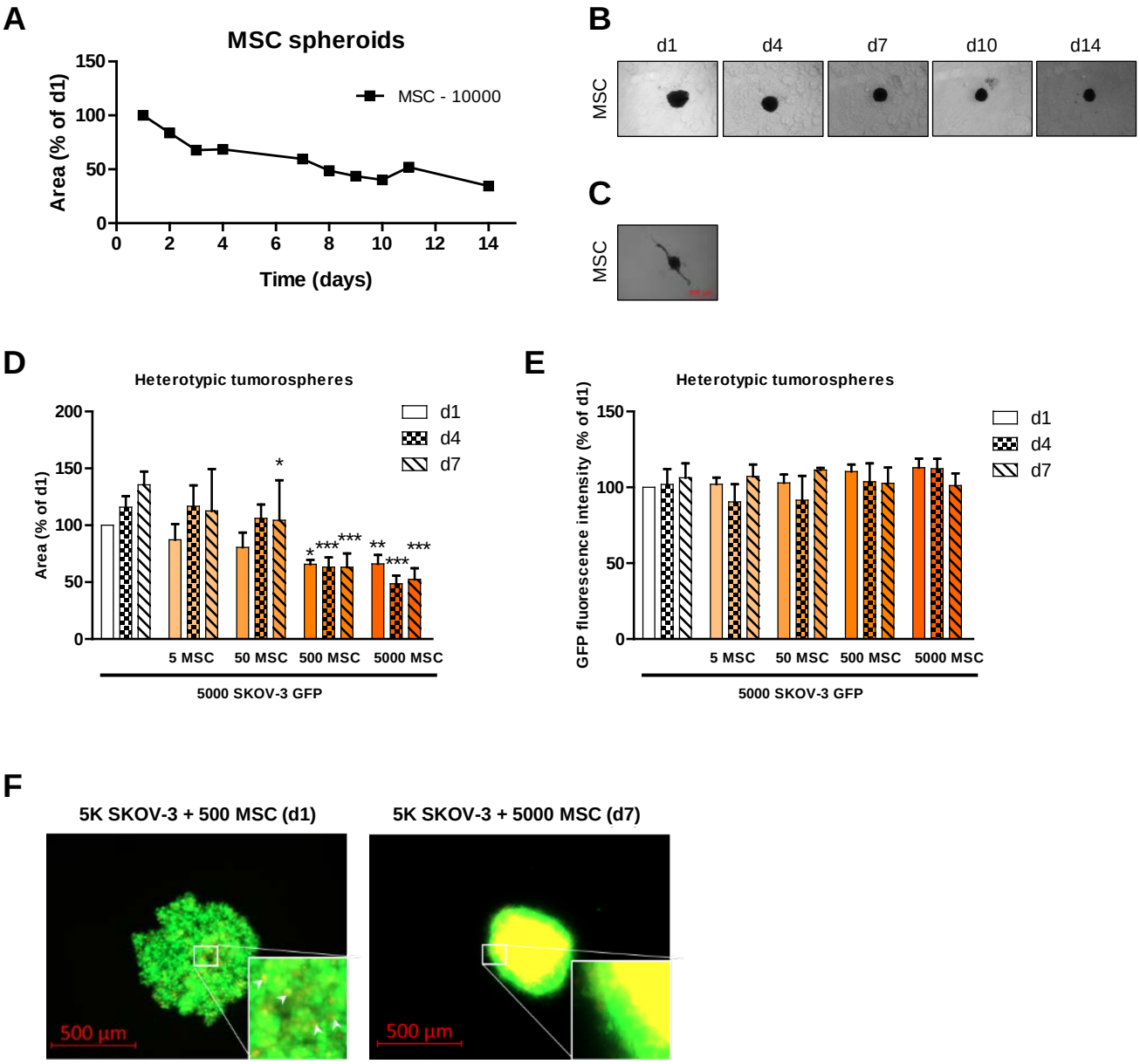

Supplementary Figure 1

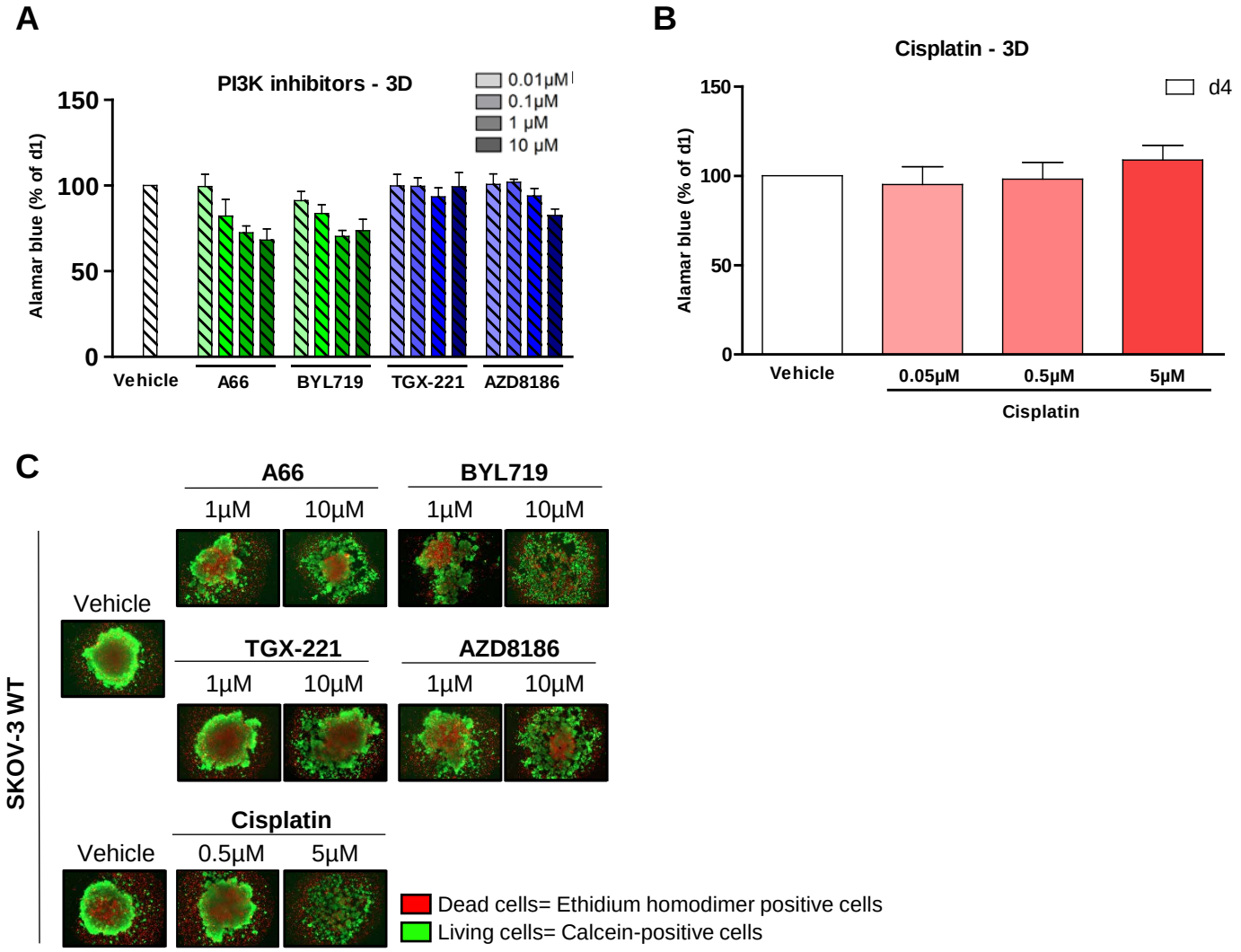

Supplementary Figure 2

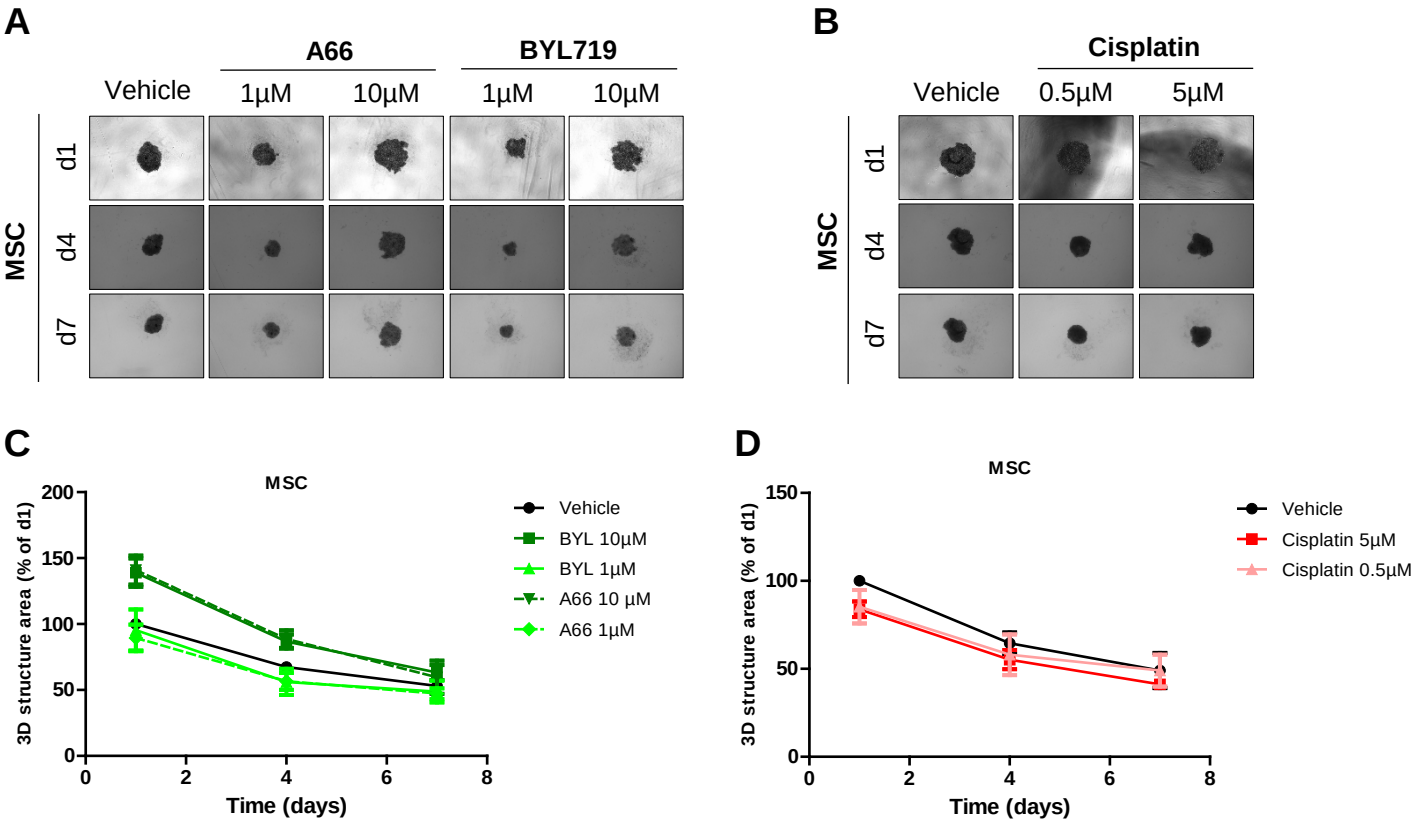

Supplementary Figure 3

Patient #	Age (years)	Histology	Aggregates number (per field)	White blood cells number (per mm³)	Normalized aggregates number	Aggregates density
1	72	high grade serous	12	350	4200	Poor
2	65	high grade serous	12	1000	12000	Rich
3	70	high grade serous	3	1350	4050	Poor
4	61	high grade serous	120	4000	480000	Rich
5	57	high grade serous	104	1300	135200	Rich
6	66	high grade serous	23	2500	57500	Poor
7	65	high grade serous	3	1200	3600	Poor
8	73	high grade serous	36	7500	270000	Poor
9	58	high grade serous	5	2500	12500	Poor
10	61	high grade serous	3	6500	19500	Poor
11	62	high grade serous	12	2950	35400	Poor
12	56	high grade serous	8	510	4080	Poor

Supplementary Table 1